Low-Cost Satellite-Based Correction Service for Precise Point Positioning in Latin America

Ramón López La Valle (iD), Ernesto López (iD), and Javier García (iD)

Abstract—Global Navigation Satellite Systems (GNSS) applications have been continuously expanding during the last years. When centimeter-level accuracy is required, the use of a single conventional GNSS receiver is not suitable because of the presence of different error sources that degrade the quality of its measurements. Precise Point Positioning (PPP) methods depend on applying corrections to significantly improve the accuracy of a single receiver allowing to obtain centimeter-level performance. This paper focuses on the design of a satellite-based service that broadcast the open access corrections for PPP generated by the International GNSS Service (IGS) being appropriate for real-time applications. The proposed system is based on the Argentinian geostationary satellite ARSAT 2 capable of providing service to Latin America. The system requirements and specifications are defined in order to deliver a good quality of service reducing the complexity and the cost of the users' receivers. Thoroughly analyzes and calculations carried out demonstrate that, adopting practical design criteria, a low-cost implementation is possible. We present the main characteristics of the uplink ground station and downlink user receivers. Moreover, different user receiver architectures as well as the design of a simple antenna are proposed. Simulation results using real data show that our solution is able to provide up to centimeter-level accuracy achieving a performance similar to other costly commercial correction services.

Index Terms—Satellite navigation systems, precise positioning, correction service, satellite broadcasting.

I. INTRODUCTION

Nowadays, many applications rely on GNSS receivers to estimate position, velocity, and time (PVT). The attainable accuracy is strongly dependent on the characteristics of the receiver and the applied techniques. Particularly, multi-frequency receivers are able to correct the ionospheric delay that is the main error source in low-cost single frequency receivers [1], [2]. On the other hand, the use of multi-constellation receivers increases the number of available satellites improving the continuity and integrity of the PVT solution in harsh environments or under adverse operation conditions [3]. This is of special interest for critical applications, where the reliability is crucial. The current fully operational systems are GPS and GLONASS, from the USA and Russia respectively.

Typically, multi-frequency and multi-constellation high-end standalone GNSS receivers can achieve meter-level accuracy due to errors in satellite orbit parameters, clock offset, and tropospheric path delay [1]. There are some applications, such as precision agriculture, geodesy, surveying, and navigation of autonomous vehicles, that need centimeter-level accuracy

Authors are with UIDET SENyT, Departamento de Electrotecnia, Facultad de Ingeniería, Universidad Nacional de La Plata, La Plata, Argentina. e-mail: lopezlavalle@ing.unlp.edu.ar.

in order to meet the specifications required to guarantee their proper operation [4].

Differential positioning that consists of combining measurements from at least two receivers is a good solution to improve the performance since common errors are canceled out [5]. The user position is estimated relative to a reference station which coordinates are well known. With the Real Time Kinematic (RTK) technique that uses carrier phase measurements it is possible to reach accuracies of few centimeters [6]. Its main drawback is related to the fact that, in order to ensure the effectivity of the corrections, the reference station should be close to the user (rover). This condition implies the necessity of installing a great number of stations to provide an adequate service coverage. Particularly, this can be difficult to satisfy in rural environments and remote places due to the associated costs.

The major disadvantages of RTK technique are overcome if a single receiver employs precise satellite orbit and clock corrections generated by a network of reference stations properly distributed around the world [7]. This method known as Precise Point Positioning (PPP) constitutes an interesting alternative to differential positioning [8], especially in locations where the deployment of RTK reference stations is not economically viable. In these cases, the corrections can be broadcast by a geostationary satellite in order to achieve a wide coverage area. The required data are provided by different companies and institutions, in particular the International GNSS Service (IGS) publishes several products depending on the quality and latency [9]. There exist products suitable for real-time applications that need centimeter-level accuracy [10]. Although the PPP convergence time is longer than RTK, this problem can be improved by using multi-constellation and especially multi-frequency receivers, thanks to the increasing number of triple-frequency satellites, which in turn can speed up the ambiguity resolution process [11], [12].

There have been some commercial services that rely on independently owned reference stations and geostationary satellites to transmit corrections for PPP using the L-band [13]–[16]. Recently, the use of low-cost receivers for PPP has been proven to be feasible [17], [18]. Nevertheless, commercial correction services are generally very expensive for potential users in development countries, where one of the main applications is precision agriculture. In [19], a correction service based on additional processing of IGS products and a regional reference network to improve the accuracy is proposed. However, the technical aspects of the broadcast of corrections is not addressed. On the other hand, it should be noted that the deployment of a regional network of stations

significantly increases the cost and complexity of the system.

In the present work, we propose the design of a system capable of providing a low-cost correction service for PPP using the Argentinian geostationary satellite ARSAT 2 that can operate in the C-band. The coverage area of this satellite makes it suitable for delivering a satisfactory service to Latin American customers. The thorough analyzes and simulations carried out demonstrate the feasibility our solution that can achieve an accuracy comparable with other expensive commercial services, being appropriate for real-time applications that demand centimeter-level accuracy. In particular, this paper is focused on the technical implementation aspects of the proposed correction service.

A preliminary market study was carried out to identify potential users as well as to estimate operation and subscription costs. With the proposed implementation, we can offer a correction service for half of the subscription cost of a commercial service with similar accuracy, which is about USD 300 per year. Indeed, with the cooperation of the Argentinian government, it will be possible to provide a free correction service in Argentina.

The rest of the work is organized as follows. Section II introduces the proposed solution and establishes the main system requirements. In Section III, the system design criteria based on practical considerations are presented. Section IV addresses the principal characteristics needed for user receivers and the uplink ground station in order to satisfy the defined requirements. Moreover, the design of the user receiver antenna as well as different possible receiver architectures are discussed. Section V presents simulation results obtained using real data. Finally, the conclusions are presented in Section VI.

II. PROPOSED SOLUTION AND SYSTEM REQUIREMENTS

The proposed system makes use of the open access corrections provided by the IGS, particularly through the IGS-RTS service, that are appropriate for real-time applications. These corrections are disseminated in a state space representation (SSR) through several standardized messages in RTCM format, depending on the chosen GNSS. Particularly, corrections for GPS satellites are transmitted every 5 seconds at a fixed rate of 1.8 kbps [20].

In our proposal, the aforementioned corrections are gathered and processed in a control center to be uploaded to the geostationary satellite by means of a ground station. End-users receive the corrections broadcast by the satellite via a downlink channel, as is shown in the simplified block diagram of the system presented in Fig. 1. This approach allows users located in remote places, without Internet connection or access to a cellular network, to obtain the corrections needed to achieve centimeter-level position accuracy. Given the state space representation in which the corrections are provided, the delay in upstream and downstream transmission is negligible from the point of view of an accuracy degradation. This PPP correction service is suitable for many applications including precision agriculture, surveying, geodesy, navigation of autonomous vehicles, and other positioning applications that require centimeter-level accuracy.
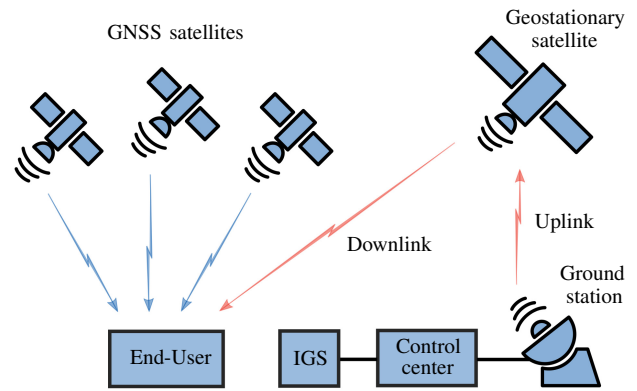

Fig. 1. Simplified block diagram of the proposed system.

There are different geostationary satellites that can be considered for this application. In particular, the Argentinian satellite ARSAT 2 is currently available and its use constitutes a strategic decision in order to avoid depending on foreign companies, which also allows to reduce the cost of the service. ARSAT 2 operates in Ku-band and C-band, while GNSS and most commercial correction services make use of the L-band. The main drawback of the Ku-band is the atmospheric attenuation, especially due to the rainfall that can compromise the system availability. In addition, the user receiver implementation becomes complicated because of the operation frequency. On the other hand, atmospheric attenuation in C-band is almost negligible as in L-band, and receiver complexity is reduced since the working frequency is considerably lower than the Ku-band. Though the adoption of C-band slightly increases the receivers complexity in comparison with the L-band alternative, as it will be shown, a low-cost system implementation is feasible.

C-band transponders of ARSAT 2 are associated to an antenna that ensures an acceptable signal level for Latin American countries [21]. In order to keep the users' receivers compact and affordable, they should be able to employ a low gain antenna with a hemispherical radiation pattern. This avoids the use of a pointing system that considerably increases the cost and complexity of the receiver. Thus, a convenient choice is a microstrip patch antenna due to its low profile, lightweight, and radiation pattern characteristics that allow to obtain a gain at C-band of about 2 dBi for the relatively low elevation angles required at high latitudes [22]. The previous condition implies a careful link budget calculation and a consequent dimensioning of both the user receiver and uplink ground station to satisfy the required signal to noise ratio.

A robust modulation scheme should be used, suggesting binary phase-shift keying (BPSK) as a suitable option. Therefore, to achieve a bit error rate (BER) of 10^{-5} needed for this application it is necessary a bit energy to noise density ratio (E_b/N_0) of 9.6 dB [23]. According to the amount of data to be transmitted and considering an overhead of around 10 % for framing and error detection through a CRC algorithm, the necessary rate (R) is estimated in 2 kbps [20].

In order to provide interference and jamming rejection, which is essential for the system reliability and signal integrity,

TABLE I
SYSTEM REQUIREMENTS.

Parameter	Value
Receiver antenna gain	2 dBi
Data modulation scheme	BPSK
Transmission technique	DSSS
E_b/N_0	9.6 dB
R	2 kbps
R_c	2 Mcps
B	2.5 MHz

we propose to use direct sequence spread spectrum (DSSS) modulation. The autocorrelation properties of the spreading code are directly related to its capability of mitigating the effects of multipath on the system performance. This feature is important for systems that rely on wide beamwidths (low gain) receiving antennas that do not have good multipath suppression characteristics. Gold codes commonly adopted in satellite communications and navigation systems are suitable for the present application. In particular, using a sequence with a chip rate (R_c) of 2 Mcps allows to obtain a processing gain of 30 dB being sufficient to effectively reduce the impact of narrow-band interference signals. A code with a sequence length of $N = 1023$ chips is chosen, similar to the GPS C/A code, facilitating the implementation of the data correction demodulation process in a GNSS receiver [24]. The code was selected to enhance the autocorrelation characteristics since in this application intercorrelation properties are less relevant because multiuser operation is not required. On the other hand, raised cosine pulse shaping is applied using a roll-off factor $\alpha = 0.25$ that greatly improves the spectral efficiency. Fig. 2a shows the simulated power spectral density (PSD) of the baseband signal without noise, which is calculated by multiplying the BPSK modulated data by the chosen spreading code and using the raised cosine pulse shaping previously defined. The autocorrelation function of the spreading code is plotted in Fig. 2b that represents one period. As it can be seen in Fig. 2a, the resulting bandwidth of the RF correction signal transmitted by the satellite (B) is 2.5 MHz. Table I summarizes the principal requirements of the system.

ARSAT 2 is a bent pipe satellite whose C-band transponders operate at center frequencies of 3981.00 MHz and 6206.00 MHz for downlink and uplink respectively [21]. The satellite relays the uplink carriers into downlink carriers, therefore the link calculation includes a combined uplink-downlink analysis.

III. LINK BUDGET

The aim of this section is to determine the main specifications of both the ground station (uplink) and receiver (downlink) based on practical criteria for guaranteeing the fulfillment of the requirements defined in Table I. The first step is a complete link analysis.

A. Link Analysis

For this system, multiple access is not needed because the same correction signal is broadcast to all users. As a
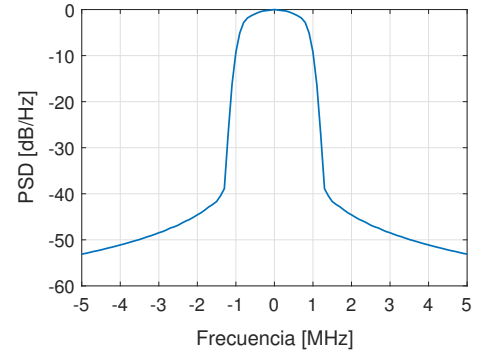
(a) Baseband PSD of the correction signal.
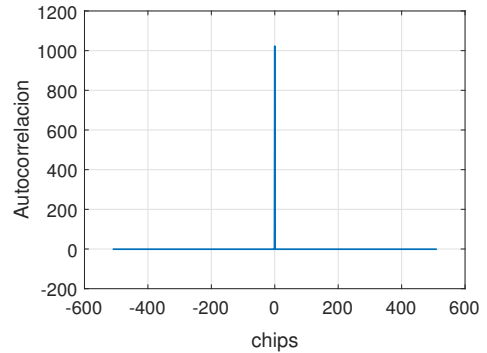
(b) One period of the autocorrelation function of the code.

Fig. 2. Power spectral density of the correction signal and autocorrelation function of the spreading code.

result, there is no interference contribution from other users allowing to carry out the link budget calculation and the system performance evaluation in the conventional way [25]. The received carrier power at the satellite is given by

$$P_r^s = \frac{EIRP_u G_r^s}{FSL_u L_a} \qquad (1)$$

where $EIRP_u = P_t^u G_t^u$ is the effective isotropic radiated power of the uplink ground station, being P_t^u the power transmitted by the uplink ground station and G_t^u the gain of the transmitting antenna. G_r^s is the gain of the satellite's receiving antenna and FSL_u is the free space loss of the uplink. Additional link losses L_a are mainly generated by five different sources: attenuation due to rainfall, gaseous absorption, clouds, pointing losses, and polarization loss. At C-band frequencies, the first three sources that define the atmospheric attenuation are almost negligible. In fact, the maximum value of the atmospheric attenuation exceeded for 0.01% of the time in the coverage area, calculated using the ITU-R propagation models software library from CNES, is about 1.2 dB. Therefore, as a worst case we will consider $L_a = 5$ dB for both uplink and downlink. It should be pointed out that the pessimistic estimate of the additional losses acts as a security margin.

The carrier power P_r^s can be written in terms of the bit energy E_b and the bit rate R as $P_r^s = E_b R$. In addition, the noise density ratio is calculated as $N_0 = kT_{sys}^s$, where k is the Boltzmann constant and T_{sys}^s is the equivalent noise temperature of the receiving satellite system. Therefore, using

(1) is possible to obtain an expression for the bit energy to noise density ratio of the uplink

$$\frac{E_b}{N_0}\bigg|_u = \frac{EIRP_u}{FSL_u L_a k R}\frac{G_r^s}{T_{sys}^s} \tag{2}$$

A similar procedure is applied to derive an expression for the bit energy to noise density ratio of the downlink

$$\frac{E_b}{N_0}\bigg|_d = \frac{EIRP_s}{FSL_d L_a k R}\frac{G_r^d}{T_{sys}^d} \tag{3}$$

where $EIRP_s$ is the effective isotropic radiated power of the satellite and FSL_d is the free space loss of the downlink. The ratio G_r^d/T_{sys}^d, being G_r^d the antenna gain and T_{sys}^d the equivalent noise temperature of the user receiver system, characterizes the capability of the receiver to detect low-level signals.

Finally, the combined E_b/N_0 of the system at the downlink receiver is given by [26]

$$\frac{E_b}{N_0} = \left[\left(\frac{E_b}{N_0}\bigg|_u\right)^{-1} + \left(\frac{E_b}{N_0}\bigg|_d\right)^{-1}\right]^{-1} \tag{4}$$

B. Link Calculations

The previous formulation allows us to determine the main parameters of the uplink ground station and the downlink receiver considering the requirements defined in Table I. In particular, we can calculate the $EIRP_u$ and the figure of merit G_r^d/T_{sys}^d that describe the receiver's sensitivity. It is noted that the values of G_r^s/T_{sys}^s and $EIRP_s$ are known since depend on the specific characteristics of the satellite.

As it can be seen in the following expression, in order to obtain numerical results, it is necessary to determine the position of the ground stations because they are needed to estimate the free space losses as

$$FSL[\text{dB}] = 92.4 + 20\log(d) + 20\log(f) \tag{5}$$

where d is the distance in km between the satellite and the corresponding ground station, and f is the frequency operation of the link in GHz.

For geostationary satellites that have equatorial circular orbits at an altitude h of about 35785 km above sea level, the distance d can be calculated as [27]

$$d = \sqrt{r_E^2 + (r_E + h)^2 - 2r_E(r_E + h)\cos(\theta)\cos(\Delta\phi)} \tag{6}$$

where r_E is the mean radius of the Earth, θ is the latitude of the ground station, and $\Delta\phi$ is the difference in longitude between the subsatellite point and the ground station.

For the current analysis, we assume the uplink ground station situated in the city of La Plata (Argentina) and, as a worst-case scenario, a receiver located at a latitude of 55° which is the highest latitude within the desired coverage area of ARSAT 2. Therefore, using (6) and (5) it is possible to determine FSL_u and FSL_d since the longitude of the subsatellite point is known. Table II presents the aforementioned data, satellite parameters [21], and results obtained for free space losses.

In the worst scenario, the minimum elevation angle in degrees measured from the horizontal at the downlink user receiver is given by

TABLE II
LOCATIONS DATA, SATELLITE PARAMETERS, AND FREE SPACE LOSS RESULTS.

Parameter	Value
Subsatellite point	$0°, -81°$
$EIRP_s$ at C-band	39 dBW
G_r^s/T_{sys}^s at C-band	-5 dB/K
Uplink ground station	$-34.906585°, -57.942231°$
User receiver limit	$-55.0°, -68.0°$
FSL_u	199.7 dB
FSL_d	196.2 dB

$$\psi = \arccos\left(\frac{d^2 + r_E - (r_E + h)^2}{2r_E d}\right) - 90° \approx 27°. \tag{7}$$

Hence, at this elevation angle the receiver antenna should have sufficient gain to avoid a degradation in the system performance. The antenna characteristics will be treated in more detail in Section IV.

Considering the minimum C-band $EIRP$ and G/T of the satellite for the desired coverage area, which are shown in Table II, the E_b/N_0 of both the uplink and downlink are computed applying (2) and (3). The obtained results are shown in the following expressions

$$\frac{E_b}{N_0}\bigg|_u [\text{dB}] = EIRP_u[\text{dBm}] - 44.1 \text{ dB} \tag{8}$$

$$\frac{E_b}{N_0}\bigg|_d [\text{dB}] = 33.4 \text{ dB} + \frac{G_r^d}{T_{sys}^d}[\text{dB/K}] \tag{9}$$

In order to guarantee the proper functioning of the link, the system E_b/N_0 given by (4) should be greater than the value specified in Table I. For this application, the limitation is in the downlink due to the low gain requirement of the user receiver antenna, which is imposed to simplify the hardware reducing its cost and size. Therefore, we defined the E_b/N_0 of the downlink 1 dB higher than the system requirement, i.e. 10.6 dB, to provide an additional security margin. This is particularly important for low elevations angles where the gain of the receiving antenna is reduced. On the other hand, the uplink E_b/N_0 was chosen to minimize its effect on the overall system performance. This can be done by setting $EIRP_u = 73$ dBm which is a value that can be easily achieved by an uplink ground station even using a small antenna.

According to the previous considerations, replacing (8) and (9) in (4) yields a system E_b/N_0 of 10.5 dB that is adequate to ensure a good quality of service. This result obtained assuming adverse propagation conditions demonstrates that the excess link margin (ELM) is at least 0.9 dB for the worst-case scenario.

IV. DESIGN OF THE GROUND STATIONS

Based on the analysis carried out before, the fundamental characteristics of both the uplink ground station and downlink user receivers are determined in this section.

A. User Receiver

Considering the target E_b/N_0 of the downlink and using (9), the necessary G_r^d/T_{sys}^d is -22.8 dB/K. The required noise figure of the receiver is calculated by

$$NF_r = 10 \log \left[1 + \left(\frac{G_r^d}{G_r^d/T_{sys}^d} - T_a \right) \frac{1}{T_0} \right] \quad (10)$$

where $T_0 = 290$ K is the reference temperature and T_a is the equivalent noise temperature of the antenna, which for this application is about 200 K. Given the gain of the receiving antenna G_r^d specified in Table I, the required receiver noise figure is $NF_r = 1.3$ dB. In order to achieve this condition, an active antenna is needed and its low noise amplifier (LNA) should have a noise figure lower than 1.3 dB and sufficient gain to minimize the contribution of the other stages of the RF chain in the total noise figure of the receiver. There exists in the market several small LNAs that meet the aforementioned requirements [28], [29], in consequence, a low-cost practical implementation is possible.

To determine the capability of the user receiver to acquire and track the correction signals, we estimate the carrier to noise density ratio C/N_0. Using the minimum resulting system E_b/N_0 and the relation between the carrier power and the data rate, the C/N_0 for the worst-case scenario is

$$\left. \frac{C}{N_0} \right|_{min} = \left. \frac{E_b}{N_0} \right|_{min} [\text{dB}] + 10 \log (R) \approx 42.5 \text{ dB-Hz.} \quad (11)$$

Certainly, this result exceeds the expected values for GNSS signals that can be properly acquired with lower C/N_0 levels.

The received correction signals can be downconverted by a low noise block (LNB) located near the antenna in the same enclosure. If the intermediate frequency is chosen within the L-band close to the carrier frequency of the GPS L1 signal, an additional channel in the GNSS receiver is capable of performing the majority of the processing required to demodulate the correction data since both systems rely on the same modulation technique. Consequently, this solution reduces the implementation complexity because all the tasks are carried out in a single receiver. On the other hand, the previously estimated C/N_0 confirms that an implementation on based on a GNSS receiver is feasible and cost-effective because the spreading codes are the same used in GPS, which permits to exploit functions already addressed in the signal processing stage. Fig. 3 is a block diagram of the C-band LNB and the GNSS active antenna operating with a dual-antenna GNSS receiver, where one channel is configured to process the correction data. It is noteworthy that the C-band antenna and the LNB can be integrated with the GNSS antenna simplifying the hardware associated with the receiver, which is of special interest in mobile applications. A programmable dual-antenna GNSS receiver of our own design that is suitable for this application is presented in [30]. The cost of this receiver is about USD 400, which is considerable lower than the cost of other commercial high-precision receivers typically used for PPP applications. On the other hand, an extra license to unlock the use of PPP corrections is not required.

A different approach consists of using an independent receiver to demodulate and implement the corrections. In this
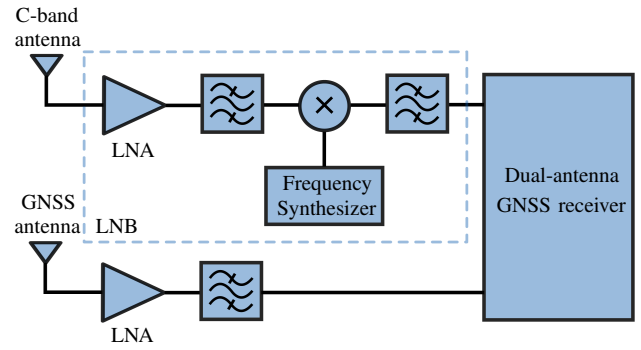
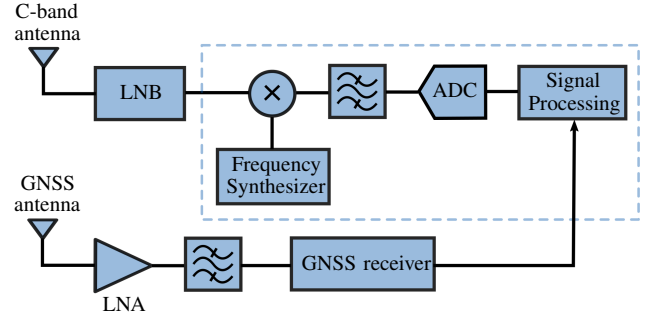

Fig. 3. Proposed system receiver block diagram.

Fig. 4. Alternative implementation using a conventional GNSS receiver.

case, a low-cost conventional GNSS receiver can be employed since the IGS-RTS service provides corrections applicable to the GNSS broadcast ephemeris [10], [17]. The main drawback of this somewhat cumbersome solution, schematized in Fig. 4, is the complicated extra hardware needed for processing the corrections that, in addition to the LNB, it should include a down-conversion stage, an analog to digital converter (ADC), and a digital signal processing block. Nevertheless, the users can take advantage of their own GNSS receivers if they generate pseudorange and carrier phase measurements.

It should be noted that even though the proposed solution could lead to an increase in the cost of the user receiver hardware in comparison with other commercial services that operate in the L-band, we can offer a subscription cost significantly lower than those services. This is because our correction service relies on the IGS products, thus we do not need to deploy and maintain a network of reference stations.

B. Receiver Antenna Design

The C-band antenna should have circular polarization in order to be able to receive the linearly polarized signals transmitted by the satellite without appreciable losses due to the relative orientation of the receiver. As it was proposed in Section 2, a microstrip patch antenna is an attractive alternative because of its advantages over other implementations. In particular, patch antennas have hemispherical radiation patterns that provide good coverage even for low elevation angles and also they can be designed to obtain circular polarization.

Microstrip patch antennas are composed of a conductor strip and a ground plane separated by a dielectric material of relative permittivity ε_r with thickness h that acts as a
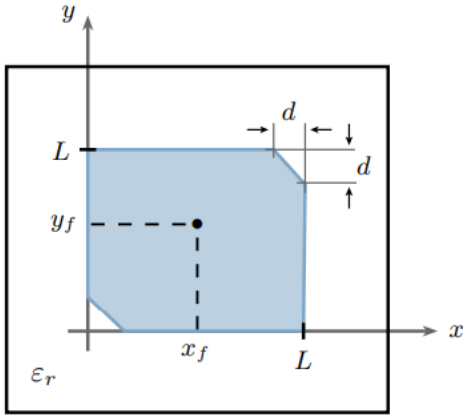
Fig. 5. Square patch circularly polarized antenna.

TABLE III
ANTENNA PARAMETERS ASSUMING RO4350B SUBSTRATE
MATERIAL.

Parameter	Value
h	1.524 mm
L	18.6 mm
d	2.8 mm
x_f	9.3 mm
y_f	13.8 mm

substrate. Though different strip shapes are possible, one of the most common implementation is the rectangular patch owing to its simplicity. In order to obtain circular polarization, two orthogonal modes with equal amplitude and in quadrature phase should be simultaneously excited. This can be done by introducing a perturbation in the patch, which allows to use a single feed point [31]. This is an additional benefit since it simplifies the design and reduces its cost. The proposed structure shown in Fig. 5 consists of a square patch with truncated corners to produce the required perturbation.

The effective length of the patch is given by

$$L_e = \frac{c}{2f_0\sqrt{\varepsilon_e}} \tag{12}$$

where c is the vacuum speed of light, f_0 is the resonance frequency defined as the carrier frequency of the downlink, and ε_e is the effective dielectric constant [22].

The effect of the fringing fields at the ends of the patch can be described in terms of an additional line length ΔL [31]. Therefore, the actual physical length of the patch is slightly smaller than the effective length given by (12).

The input impedance at the dominant resonant mode depends on the position of the feed point. In the proposed design, a coaxial feed is used for simplifying the connection with the rest of the circuits. The location of the feed point (x_f, y_f) is chosen to obtain impedance matching between the antenna and the feed line, whose characteristic impedance is 50Ω. The length of the patch L is approximately calculated using equation (12).

For the present implementation, we chose the low cost hydrocarbon ceramic laminate RO4350B which has a nominal dielectric constant $\varepsilon_r = 3.48$ [32]. This material is suitable for the downlink frequency operation and exhibits low dielectric losses. The length of the patch, the position of feed point, and the distance d for the truncated corners were estimated and optimized by performing electromagnetic simulations using Altair Feko™ including dielectric and metallic losses to achieve more realistic results. The obtained values are shown in Table III.

Fig. 6a presents the simulated S_{11} parameter of the antenna that is a measure of its impedance matching. A S_{11} value below -10 dB indicates that the matching is satisfactory,

therefore the proposed design is capable of operating at the downlink frequencies with good impedance matching reducing the losses due to the reflected power at the antenna input. The simulated axial ratio at the downlink carrier frequency is plotted in Fig. 6b, where it can be seen that the circular polarization performance is appropriate even at low elevation angles since the axial ratio is lower than 3 dB. This minimizes the polarization loss improving the downlink signal-to-noise ratio.

Two orthogonal cuts of the simulated realized gain pattern are presented in the polar plot of Fig. 7. The symmetry of both cuts demonstrates the hemispherical characteristic of the achieved radiation pattern. The maximum gain (zenith) is about 6 dBi and the 3 dB beamwidth is 95°.

For this application, the gain at the lowest required elevation angle measured from the horizontal $\psi \approx 27°$, equivalent to $\theta \approx 63°$, is about 1 dBi. Using the actual antenna gain in (9), instead of the 2 dBi assumed before, and considering a receiver with a noise figure of 1.3 dB according to the results presented in Section 3, the system E_b/N_0 calculated by substituting (8) and (9) in (4) is approximately 9.6 dB. This value still meets requirement defined in Table I, thus the simple and low cost antenna design proposed is suitable for receiving the correction signals providing a satisfactory quality of service in the whole coverage area of interest. It is noted that for lower latitudes the system operates with a considerable ELM since the typical gain of the antenna is higher than 2 dBi, which increases the real G/T of the user receiver.

The size of designed antenna is only 30 mm $\times$ 30 mm, which demonstrates that user receiver hardware miniaturization is attainable. On the other hand, a variety of compact GNSS antennas have been proposed by other authors and different models are currently available in the market [33], [34]. As it was mentioned before, it is possible to place both the C-band and GNSS antennas into the same enclosure that can also accommodate the LNB. This contributes to further reduce the size of the receiver system.

C. Uplink Ground Station

Considering the desired $EIRP$ of the uplink ground station obtained in Section 3, it is possible to determine the necessary gain of the antenna and the power to be transmitted by defining some practical constraints. The gain of a parabolic antenna normally used in this kind of applications depends on its diameter D. For a given operation frequency, the only way of achieving a high gain is by increasing the diameter of
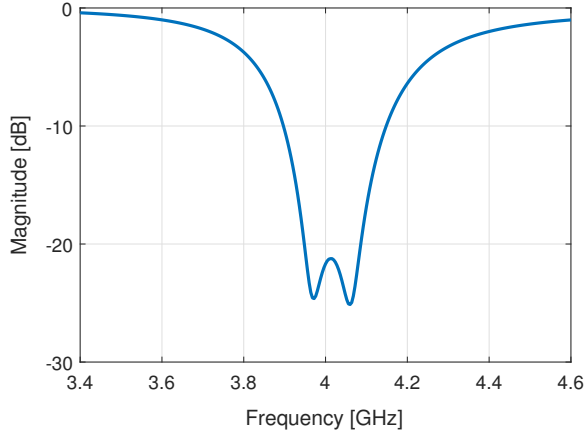
(a) Simulated S_{11} parameter of the antenna.
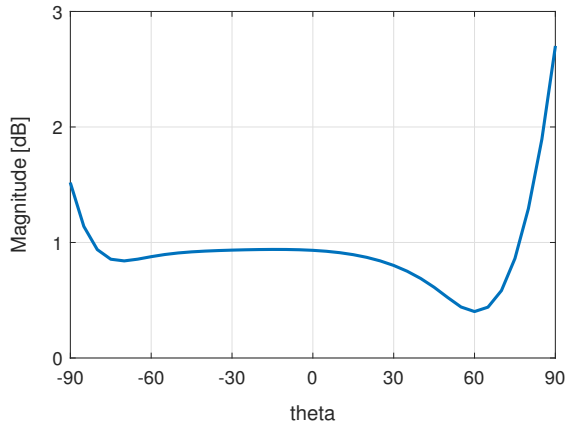
(b) Simulated axial ratio at downlink carrier frequency.
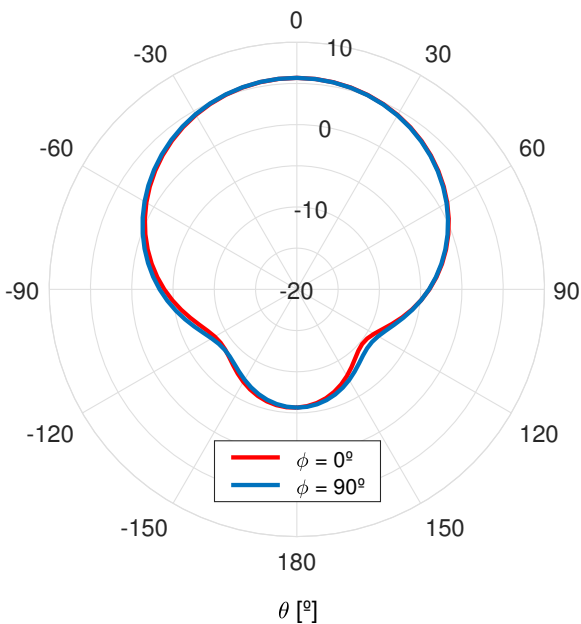
Fig. 6. Simulation results for the S_{11} parameter and the axial ratio of the antenna.

Fig. 7. Simulated realized gain at downlink carrier frequency.

the antenna which elevates its cost. On the other hand, there exist limitations in the minimum size since small antennas transmitting in C-band can create high interference due to side lobes.

The use of a low gain antenna implies a higher transmitted power P_t^u in order to obtain the desired $EIRP$. The cost and complexity of a high-power amplifier are relevant, especially for output powers greater than 10 W (40 dBm). To keep the output power below this limit, the corresponding diameter of the antenna is chosen. For a standard size $D = 1.8$ m, which is appropriate for C-band operation, the gain is $G_t^u \approx 39$ dBi. With this election the minimum output power is

$$P_t^u = EIRP_u - G_t^u = 34 \text{ dBm} \tag{13}$$

which is equivalent to 2.5 W, and hence satisfies the condition imposed before.

The power amplifier can be built with a GaN device suitable for handling the power to be transmitted by the uplink ground station. An alternative approach consists of using a commercial block up-converter (BUC) that typically converts an incoming modulated L-band signal to the C-band delivering the required output power, which in this application is low. In both cases, the ground station may be entirely based on a software defined radio (SDR) platform that generates the modulated C-band signal for the power amplifier or the L-band signal needed for the BUC. This constitutes a versatile and economical way of implementing the ground station, and hence confirms the feasibility of the proposed solution in terms of easy implementation and low cost.

V. RESULTS

In order to assess the improvement in the positioning accuracy achieved by the use of the proposed correction service, we present an application example using real data obtained from IGS GNSS stations. For this analysis, measurements were processed from four stations, located in Argentina (CORD), Brazil (CHPI), Peru (AREG), and Colombia (BOGT), representative of the planned coverage area. These stations are equipped with high-precision GNSS receivers providing dual-frequency pseudorange and carrier-phase measurements. The Precise Point Positioning was carried out according to [10], performing a daily estimation of the three position coordinates by means of a statistical filtering of the dual-frequency GPS measurements combined in the linear ionosphere-free combination [2]. For each station, measurements corresponding to a full week of March 2020 were processed. These are available daily in RINEX format through the CDDIS repository [35].

The processing was done in three steps. First, the final orbits and clocks products, provided by the IGS in SP3 format [36], were used in order to obtain a reference position against which to contrast the results of the real-time oriented processing. In second place, the broadcast ephemerides transmitted in the navigation message were used as a real-time case processing without any corrections. Finally, the PPP corrections were used to obtain a real-time high-precision solution. Although in both cases, the GPS data was not used in real-time but obtained in RINEX format in the ephemerides case and through the IGC
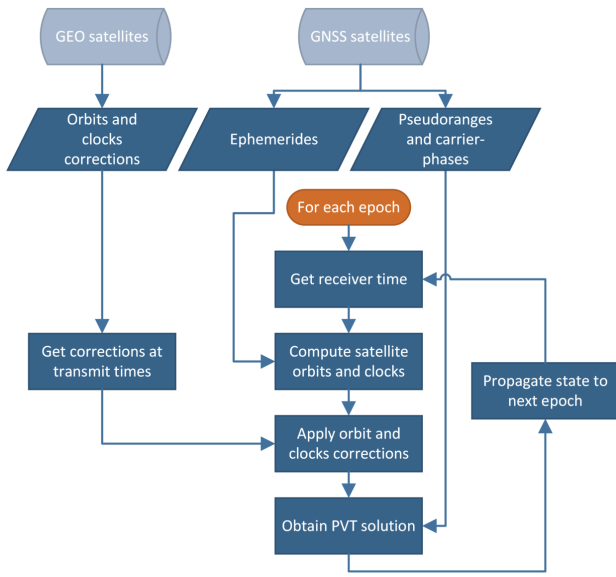
Fig. 8. Workflow of the operation of a receiver.

products, which contains the correction data streams decoded in SP3 format, the processing scheme applied was the same as it would be in a real-time application. As mentioned in Section 2, the SSR corrections are provided every 5 seconds. In case of data gaps or a decrease in temporal resolution, this representation allows its extrapolation with a minimal accuracy degradation, mainly caused by the satellite clock prediction. However, since the corrections already decoded and applied were used for this processing, the results presented are representative only for the nominal message rate. A simple workflow diagram of the operation of a receiver capable of demodulating these corrections is shown in Figure 8. In the previous case, with a receiver working only based on ephemerides, the only difference to this scheme would be the absence of the blocks of calculation and application of the corrections.

The last estimate of the PPP solution with final products was used as reference to calculate the error in East-North-Up coordinates (E, N, U) for both real-time solutions. Figs. 9a and 9b show the horizontal and vertical position error, respectively, for CORD station during 24 hours for each type of product. While the solution obtained with ephemerides (blue) never fully converges to the reference position, it can be seen that the solution with the corrections applied (orange) exhibits a behavior similar to that obtained by post-processing with final products (black).

For the real-time processing using corrections, a convergence time between 20-45 minutes depending on the station, the visibility of GNSS satellites, and the constellation geometry, was observed. The convergence time is evaluated considering a threshold of 0.5 m error in the horizontal plane. On the other hand, the results obtained using ephemerides simply do not achieve enough precision to define a convergence time. A summary of the results for each station is presented in Table IV, depicting the week mean RMS error, excluding the convergence time, as well as the maximum daily RMS error. Overall, a sub-decimeter and decimeter level was observed in
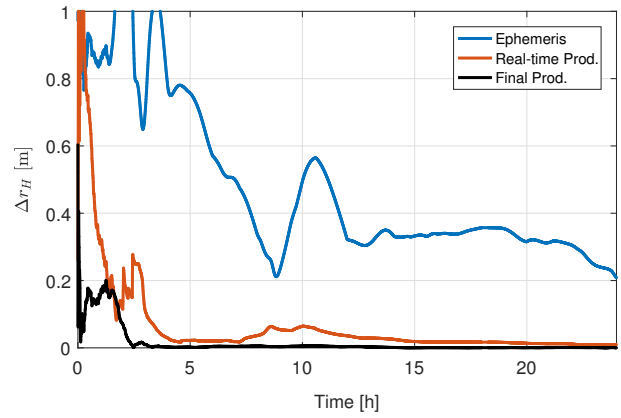
(a) Horizontal position error.
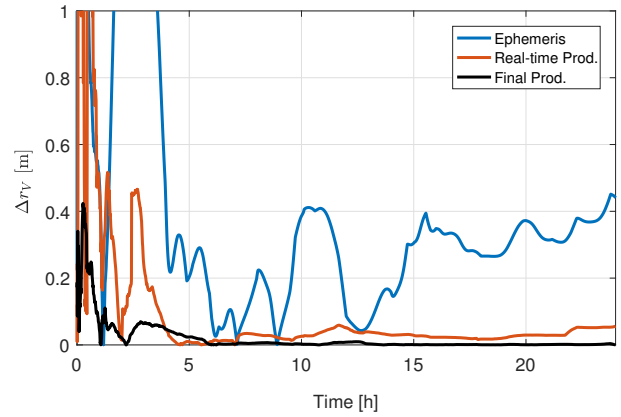
(b) Vertical position error.

Fig. 9. Horizontal and vertical position error for the CORD station.

the horizontal and vertical plane respectively, representing a precision improvement of up to 6 with respect to the solution using ephemerides.

The RMS horizontal accuracy achieved by applying the real-time corrections is about 8 cm. This outstanding performance is superior to some of the existing well-known commercial services, as is shown in Table V. It should be mentioned that Table V was built based on data published by the service providers, which is available on-line [37]–[40]. The statistics of some of these commercial services correspond to the use of multi-GNSS corrections, in which case the convergence time decreases notably, while the precision increases. For this application example only GPS corrections were used, with the available measurements from the mentioned stations. If multi-GNSS corrections are transmitted and receivers capable of operating with them are used, convergence time and accuracy could be improved.

VI. CONCLUSIONS

The complete design of a satellite system capable of providing a low-cost correction service for PPP was presented. The service is based on a geostationary satellite that broadcast the open access correction data generated by the IGS, which are suitable for real-time applications. This enables to obtain centimeter-level accuracy for users located in Latin America.

TABLE IV
RESULTS FOR EACH STATION, WHERE (E, N, U) ARE EAST-NORTH-UP COORDINATES.

Product	Station	Mean RMSE			Max RMSE		
		E [cm]	N [cm]	U [cm]	E [cm]	N [cm]	U [cm]
Ephemerides	AREG	28.0	9.5	34.9	39.9	10.7	45.4
	CORD	39.9	12.7	33.0	54.4	22.1	56.8
	CHPI	24.4	12.0	44.2	33.3	22.2	57.9
	BOGT	36.6	9.8	32.6	42.1	16.1	65.2
Corrections	AREG	6.1	4.4	13.7	7.7	9.7	27.1
	CORD	7.2	3.3	10.1	9.9	7.4	12.2
	CHPI	4.0	2.0	7.2	7.6	3.8	11.8
	BOGT	9.5	3.9	15.3	19.4	5.6	34.2

TABLE V
COMPARISON BETWEEN DIFFERENT SERVICES.

Service	Product	Horizontal accuracy [cm]	Vertical accuracy [cm]	Convergence time [min]
TerraStar	L	40	60	<5
	C	4	6.5	30
	C-Pro	2.5	5	<18
Atlas	Basic	30	N/A	
	H30	15	N/A	10-40
	H10	4	N/A	
Trimble	ViewPoint	50	N/A	
	RangePoint	30	N/A	<20
	FieldPoint	10	N/A	
	CenterPoint	2	5	
This work		7.8	14.6	20-45

The proposed system makes use of the Argentinian satellite ARSAT 2 which have C-band transponders appropriated to transmit the needed corrections. This could slightly increase the cost of the user receiver hardware in comparison with other commercial services that operate in the L-band. However, the nonrecurring cost is compensated by offering a very low subscription fee because with our proposal we do not need to deploy and maintain any reference station. This makes it a valuable option specially for development countries where potential users cannot afford the cost of other available services. Indeed, our solution allows us to provide a correction service for about half of the superscription cost of a commercial service with similar accuracy.

The approach adopted for planning the system and defining the requirements was based on reducing the complexity of the user receiver, while ensuring a satisfactory quality of service in the desired coverage area. In this way, we proposed to use low gain hemispherical antennas for receiving the corrections in order to avoid the necessity of pointing devices that increase the cost and size of the receivers, which is particularly inconvenient for mobile applications. On the other hand, the spread spectrum modulation chosen allows to mitigate the effects of multipath and provides rejection to interferences, which is crucial for the system reliability. The specifications of the uplink ground station and the downlink user receivers were determined taking into account the established requirements and practical considerations to facilitate their implementation. We presented a user receiver architecture that employs a LNB to down-convert the C-band signals into L-band and a low-cost configurable dual-antenna GNSS receiver, where one channel is used to demodulate the corrections that are applied to the GNSS ephemerides produced by the other channel. Also, the design of a simple C-band microstrip circularly polarized patch antenna was proposed.

The obtained results demonstrate the feasibility of a low-cost practical implementation of a system capable of improving the positioning accuracy to centimeter-level, similar or even better than other expensive commercial services. In particular, the RMS horizontal accuracy achieved by applying the proposed corrections is about 8 cm.

REFERENCES

[1] C. Hegarty, E. Kaplan, M. Uijt de Haag, and R. Cosentino, "GNSS errors," in *Understanding GPS/GNSS: Principles and Applications* (E. Kaplan and C. Hegarty, eds.), ch. 10, pp. 619–658, Norwood, MA: Artech House, 3 ed., 2017.
[2] J. Sanz Subirana, J. Juan Zornoza, and M. Hernández-Pajares, *GNSS Data Processing*, vol. 1. Noordwijk, Netherlands: ESA Communications, 2013.
[3] N. Zhu, J. Marais, D. Bétaille, and M. Berbineau, "GNSS position integrity in urban environments: A review of literature," *IEEE Trans. Intell. Transp. Syst*, vol. 19, no. 9, pp. 2762–2778, 2018.

[4] European Global Navigation Agency, "GSA GNSS Market Report," 2019.

[5] S. Bisnath, M. Uijt de Haag, D. Diggle, C. Hegarty, D. Milbert, and T. Walter, "Differential GNSS and precise point positioning," in *Understanding GPS/GNSS: Principles and Applications* (E. Kaplan and C. Hegarty, eds.), ch. 10, pp. 709–784, Norwood, MA: Artech House, 3 ed., 2017.

[6] D. Odijk and L. Wanninger, "Differntial positioning," in *Springer Handbook of Global Navigation Satellite Systems* (P. Teunissen and O. Montenbruck, eds.), ch. 10, pp. 753–780, Cham, Switzerland: Springer, 2017.

[7] J. Zumberge, M. Heflin, D. Jefferson, M. Watkins, and F. Webb, "Precise point positioning for the efficient and robust analysis of GPS data from large networks," *Journal of Geophysical Research*, vol. 102, no. B3, pp. 5005–5017, 1997.

[8] C. Rizos, V. Janssen, C. Roberts, and T. Grinter, "Precise point positioning: Is the era of differential GNSS positioning drawing to an end?," in *FIG Working Week 2012*, May 2012.

[9] J. Kouba and P. Héroux, "Precise point positioning using IGS orbit and clock products," *GPS Solutions*, vol. 102, pp. 12–28, 2001.

[10] M. López, S. Rodríguez, J. García, and C. Muravchik, "Performance comparison of precise point positioning using real-time oriented GNSS products," in *2019 Argentine Conference on Electronics (CAE 2019)*, pp. 52–57, March 2019.

[11] P. Li and X. Zhang, "Integrating GPS and GLONASS to accelerate convergence and initialization times of precise point positioning," *GPS Solutions*, vol. 18, pp. 461–471, 2014.

[12] D. Laurichesse and A. Blot, "Fast PPP convergence using multi-constellation and triple frequency ambiguity resolution," in *29th Int. Tech. Meeting Satell. Div. Inst. Navig. (ION GNSS+ 2016)*, pp. 2082–2088, Sept. 2016.

[13] Hemisphere, "Atlas® GNSS Global Correction Service," 2020.

[14] NovAtel, "TerraStar® Global Correction Services: Global Correction Services," 2019.

[15] C. Wang and R. Hatch, "StarFire® GNSS: The Next Generation StarFire Global Satellite Based Augmentation System," 2012.

[16] Trimble, "OmniSTAR® Services that Covers the Earth," 2012.

[17] Z. Nie, F. Liu, and Y. Gao, "Real-time precise point positioning with a low-cost dual-frequency GNSS device," *GPS Solutions*, vol. 24, no. 9, pp. 1–11, 2019.

[18] L. Wang, Z. Li, N. Wang, and Z. Wang, "Real-time GNSS precise point positioning for low-cost smart devices," *GPS Solutions*, vol. 25, no. 69, pp. 1–13, 2021.

[19] P. Zhou, *Low-Cost Real-Time Precise Point Positioning (PPP) Correction Service with High Availability and Accuracy*. PhD thesis, University of Calgary, 2020.

[20] International GNSS Service, "IGS Real-Time Service," 2013.

[21] ARSAT, "ARSAT 2 Prestaciones Generales," 2019. rev. 1.

[22] C. Balanis, *Antenna Theory: Analysis and Design*. Hoboken, NJ: John Wiley & Sons, 4 ed., 2016.

[23] S. Haykin, *Digital Communication Systems*. Hoboken, NJ: John Wiley & Sons, 2013.

[24] Global Positioning Systems Directorate, "IS-GPS-200 NAVSTAR GPS Space Segment/Navigation User Segment Interfaces," 2019.

[25] T. Nguyen and C. Wang, "On the link budget calculation for cdma systems," in *2001 IEEE Aerospace Conference Proceedings Proceedings*, pp. 2/909–2/913, March 2001.

[26] R. Gagliardi, *Satellite Communications*. New York, NY: Van Nostrand Reinhold, 2 ed., 1991.

[27] R. Freeman, *Radio System Design for Telecommunications*. Hoboken, NJ: John Wiley & Sons, 3 ed., 2007.

[28] Skyworks Solutions Inc., "SKY67183-396LF: 400 to 6000 MHz Broadband Low-Noise Amplifier," 2020.

[29] "BGB707L7ESD General Purpose LNA MMIC with Integrated ESD Protection and Active Biasing," 2018.

[30] S. Rodríguez, J. García, G. Scillone, J. Díaz, M. López, and R. López La Valle, "Dual-antenna dual-band high performance cubesat-compatible GPS receiver," *IEEE Latin America Transactions*, vol. 18, no. 2, pp. 265–272, 2020.

[31] P. Bhartia, I. Bahl, R. Garg, and A. Ittipiboon, *Microstrip Antenna Design Handbook*. Norwood, MA: Artech House, 2001.

[32] Rogers Corporation, "RO4000® Series High Frequency Circuit Materials," 2018.

[33] J. Wang, "Antennas for global navigation satellite system (GNSS)," *Proc. IEEE*, vol. 100, no. 7, pp. 2349–2355, 2012.

[34] Nasimuddin, X. Qing, and Z. N. Chen, "A compact circularly polarized slotted patch antenna for GNSS applications," *IEEE Trans. Antennas Propag.*, vol. 62, no. 12, pp. 6506–6509, 2014.

[35] Crustal Dynamics Data Information System, "International GNSS service, daily 30-second observation data." Available: http://cddis.gsfc.nasa.gov/Data_and_Derived_Products/GNSS/daily_gnss_o.html, Oct. 2020.

[36] International GNSS Service, "IGS products." Available: https://kb.igs.org/hc/en-us/articles/115003935351, Oct. 2020.

[37] NovAtel, "TerraStar correction services." Available: https://novatel.com/products/gps-gnss-correction-services/terrastar-correction-services/compare-terrastar-services, March 2022.

[38] Hemisphere, "Atlas® GNSS global correction service." Available: https://www.hemispheregnss.com/product/atlas-gnss-global-correction-service, March 2022.

[39] Trimble, "RTX correction service." Available: https://help.trimblegeospatial.com/TrimbleAccess/latest/en/GNSS-survey-RTX.htm, March 2022.

[40] Trimble, "Accuracy chart." Available: https://positioningservices.trimble.com/wp-content/uploads/2019/02/accuracy_chart.pdf, March 2022.

Ramón López La Valle received the Electronics Engineering and the M.Sc. in Engineering degrees from the National University of La Plata (UNLP), Argentina, in 2008 and 2014, respectively. He is currently an Assistant Professor with the UNLP, involved in research and development of Global Navigation Satellite Systems (GNSS) receivers for aerospace applications. His research interests include electromagnetic compatibility, antennas, and radio frequency and microwave circuits with applications to GNSS and wireless communications.

Ernesto López received the Electronics Engineering degree from the National University of La Plata (UNLP), Argentina, in 2015. He is currently pursuing the Ph.D. degree in Electronics Engineering at UNLP. His research interest includes statistical signal processing applied to the development of high precision GNSS-based positioning techniques, and precise orbit and baseline determination for satellite navigation.

Javier García received the Electronics Engineering degree from the National University of La Plata (UNLP), Argentina, in 2003. He is currently a Professor in the UNLP, involved in research and development of Global Navigation Satellite Systems (GNSS) receivers and processing techniques for aerospace and high-precision applications. His interests are in Statistical Signal Processing, Digital Communications, and Embedded Systems with applications to GNSS.